Powder Metallurgy (2011). 54(4), 543-550.
DOI: http://dx.doi.org/10.1179/003258910X12827272082623

Influence of powder characteristics on sintering behaviour and properties of PM Ti alloys produced from prealloyed powder and master alloy

L. Bolzoni*, P. G. Esteban, E. M. Ruiz-Navas and E. Gordo

Departamento de Ciencia e Ingeniería de Materiales e Ingeniería Química, Universidad Carlos III de Madrid, Avda. de la Universidad, no. 30, Leganés, Madrid 28911, Spain

* Corresponding author, email lbolzoni@ing.uc3m.es

Abstract: The use and development of titanium and titanium alloys have been strongly correlated to high technology industries where costs are not the most important aspect. Titanium could see its market grow by the application of lower cost and more efficient processing methods such as powder metallurgy. This work deals with the characterisation of two types of powders: commercial prealloyed powder and powder produced from master alloy combining mechanical milling and conventional blending to adjust the particle size. The characteristics of the powders, sintering behaviour and final properties of the parts indicate that the master alloy approach leads to better compressibility than the prealloyed powders and, therefore, to lower dimensional change during sintering. The most important result is that it is possible to obtain Ti alloys with properties similar to or better than alloys from prealloyed powders and to obtain homogeneous microstructures, which allows the composition to be adjusted to requeriments.

Keywords: PM Ti, Ti–6AI–4V, Ti–3A–2·5V, Prealloyed, Master alloy, Sinterability

Introduction

Since Kroll found out a process to reduce titanium ore into the pure metal,[1] there have been many attempts to develop a more efficient and less costly reduction process, but both the Kroll and the Hunter processes, the latter a variant of the former process that employs Na instead of Mg,[2] remained for many years as the only options to obtain titanium in metallic form. However, new processes have been developed in the last two decades, such as the International Titanium Powder/Armstrong process[2,3] and the Fray–Farthing–Chen Cambridge process,[4] also known as the electrodeoxidation process.[5]

Titanium is the fourth most abundant structural metal and has an outstanding combination of properties that include the highest strength/density ratio, excellent biocompatibility and corrosion resistance. Nevertheless, titanium and titanium alloys are still employed mostly in high technology industries where the final cost is not the most important issue. Titanium can be forged or wrought by standard techniques, but it may be also processed by means of powder metallurgy (PM) methods. Actually, PM processes have been employed for the fabrication of titanium products since the 1970s,[6] but were conditioned by the high extraction cost of the Kroll's process.

Among the titanium powder production processes, the plasma atomisation and the hydride–dehydride (HDH) processes are two of the most commonly employed for manufacturing titanium alloy powders.[7] Plasma atomised spherical powders are suitable for advanced PM techniques, such as hot isostatic pressing or metal injection moulding.[8] The HDH route is a milling process applicable for the fabrication of titanium powders[9] that relies on the crushing of relatively brittle material to obtain irregular or angular powder suitable for rigid die consolidation.

There are essentially two classical PM approaches: prealloying (PA) and blending elemental. The combination of the conventional cold uniaxial pressing and sintering route with the blending elemental approach results in the most economic way to obtain PM titanium components.[10] The use of master alloys instead of elemental powders is a lower cost way to introduce the alloying elements, but the characteristics of the raw materials have to be modified to be processed by conventional PM methods.

There has already been some researches on using the blending elemental approach to obtain titanium alloys, mainly Ti–6Al–4V, starting from either titanium sponge powder or titanium hydride with particle sizes lower than 100 μm,[11–14] or 150 μm.[15,16]

In this work, two compositions, Ti–6Al–4V and Ti–3Al–2·5V, were prepared by combining mechanical milling and conventional blending to obtain the composition required to study the influence of the

powder production route on the properties of the powder, as well as the applicability of the conventional press and sinter process to titanium PM products.

Experimental

Materials

For this study, two titanium alloys were selected: Ti–6Al–4V, for which the alloy produced by conventional ingot metallurgy has been well studied, and Ti–3Al–2·5V. The Ti–6Al–4V alloy was produced from two types of powders: a commercial HDH prealloyed powder containing the final composition required (Ti64-PA) and by conventional blending of elemental Ti powder, elemental Al powder and a commercial Al/V alloy (Ti64-MA). The preparation is described in more detail in the next section. Table 1 shows the composition and physical properties of the elemental powders and master alloy used, as provided by the suppliers; further characterisation was performed as described in the section on 'Preparation and characterisation of powders'. The same powders were used for preparing the Ti–3Al–2·5V alloy by conventional blending with HDH Ti powder.

Preparation and characterisation of powders

For the preparation of the Ti–6Al–4V alloy, an Al/V master alloy was used, whose big particle size (<6·3 mm) was reduced by means of high energy milling (HEM). For the milling step, the right ratio of Al/V alloy, elemental Al spherical powder, a small amount of elemental HDH Ti powder and the grinding media (tungsten carbide balls) were loaded into a tungsten carbide container. Milling was carried out in a Fritsch pulverisette mill under an inert gas atmosphere (Ar) to avoid or at least minimise oxidation and nitridation during milling, and a ball/powder weight ratio of 5 : 1 and speed of 400 rev min^{-1} were used. To prevent welding of the powder to the vessel or to the grinding media, a small amount of wax (1% of the total weight) was added as a process control agent (PCA). During this part of the study, powder samples were collected every 15 min for up to 2 h to measure the particle size distribution. The optimum milling time was determined to be 1 h, which led to powders with the correct ratio of Al/V (60 : 40) and particle size smaller than 63 μm. This powder was considered to be suitable for blending with the elemental Ti powder to produce the Ti–6Al–4V alloy. The conventional blending step was carried out in a Turbula mixer for 30 min.

The Ti–3Al–2·5V alloy was produced by blending elemental HDH Ti powder with the Ti–6Al–4V HDH prealloyed powder to form the Ti32 prealloyed (Ti32-PA) powder and with the Al/V master alloy (60 : 40) produced by HEM to form the Ti32 master alloy (Ti32-MA) powder. In both cases, the blending was performed in a Turbula mixer for 30 min.

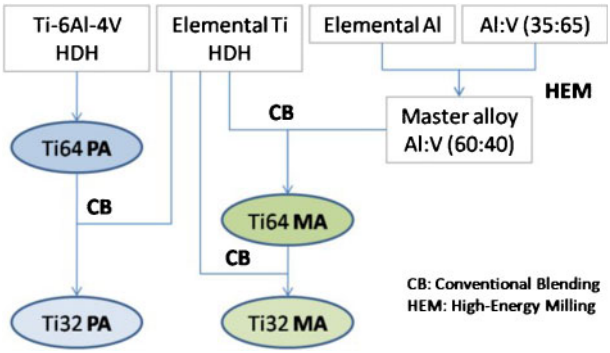

1 Scheme of powder production route employed to fabricate Ti–6Al–4V and Ti–3Al–2·5V titanium alloys

Figure 1 shows a scheme of the powder production route employed, including the raw materials and mixing techniques. It is important to remember that HEM was only used to grind the Al/V (35 : 65) master alloy to reduce its particle size distribution and adjust its composition to be mixed with pure titanium.

The powders used as raw materials and the powders prepared were characterised by different techniques: a Mastersizer 2000 laser beam analyser was used to determine the particle size distribution, a LECO TC 500 was used to measure the content of O (ASTM E 1409) and N (ASTM E 1937), and a LECO CS 200 was used to measure the content of C (ASTM E 1941). Helium pycnometry was used to obtain the density of the powder, and a Hall (MPIF 04) or a Carney (MPIF 28) apparatus was used to measure the apparent density and the flowrate (MPIF 03).

Optical microscopy and scanning electronic microscopy (SEM) were also used to study the particle shape and microstructure. Other important properties, such as the compressibility (MPIF 45) and the green strength (MPIF 15), were measured by ranging the consolidation pressure from 300 to 700 MPa using a conventional hydraulic uniaxial press to prepare the specimens.

Powder metallurgy processing and characterisation of sintered materials

The powders were uniaxially pressed into rectangular shaped specimens by means of a floating die using zinc stearate as die wall lubricant and the most appropriate pressure previously determined. A sinterability study was carried out by varying the processing temperature from 900 to 1400°C and keeping the dwell time constant at 2 h. Samples were sintered in a tubular furnace under

Table 1 Chemical composition and physical properties of starting powders (suppliers' specifications)

	Element, wt-%									
Material	Ti	Al	V	O	N	H	C	Fe	Shape	Size, μm
Ti–6Al–4V (HDH)	88·85	6·62	4·57	0·55*	0·5*	0·3*	…	0·02	Irregular	<75
Pure Ti (HDH)	99·6	…	…	0·31	0·008	0·005	0·007	…	Irregular	<75
Al/V (35 : 65)	…	35†	65†	0·300*	0·050*	0·020*	0·050*	0·500*	Irregular	<6·3
Pure Al (atomised)	…	99	…	…	…	…	…	…	Spherical	<150

*Maximum values.
†Mean values.

Table 2 Physical, chemical and technological properties of titanium alloy powders

Ti alloys		Ti64-PA	Ti64-MA	Ti32-PA	Ti32-MA
Production method		PA*	MA†	PA*	MA†
Morphology		Irregular	Irregular	Irregular	Irregular
Particle size analysis	D_{max}, μm	<75	<106	<90	<90
	D_{10}, μm	12·67	17·85	16·25	17·22
	D_{50}, μm	31·78	42·94	38·79	39·00
	D_{90}, μm	69·44	95·17	78·63	79·65
Chemical analysis	O, wt-%	0·418	0·428	0·402	0·337
	N, wt-%	0·0072	0·0121	0·0101	0·0118
	C, wt-%	0·0124	0·1050	0·0120	0·0666
ρ_{He}‡, g cm^{-3}		4·4146	4·3702	4·4560	4·4410
ρ_{app} Hall§, g cm^{-3}		…	…	…	…
Flowrate, s/50 g		…	…	…	…
ρ_{app} Carney§, g cm^{-3}		1·47±0·008	1·84±0·006	1·48±0·006	1·91±0·006

*Prealloyed.
†Master alloy addition.
‡Density measured by He pycnometry.
§Apparent density by Hall or Carney.

a vacuum level of $\sim 10^{-5}$ mbar using a heating and cooling rate of 5°C min^{-1}.

The sintered samples were characterised in terms of relative density, dimensional change (MPIF 44) and microstructure. Moreover, mechanical properties, such as the HV30 hardness, transverse rupture strength (TRS) and flexural strain, as measured by the three-point bending test (MPIF 41), were also determined.

Results and discussion

Powder characterisation

Table 2 summarises the particle size distributions, interstitial element contents (oxygen, nitrogen and carbon), densities and flow properties of the powders.

From Table 2, it can be seen that the four powders have similar particle size distributions, i.e. similar values of D_{10}, D_{50} and D_{90} where the commercial prealloyed powder Ti64-PA has the smallest particle size (<75 μm).

Nitrogen content is ~0·01 wt-%, and oxygen content is ~0·4 wt-% for all the alloys except for the Ti32-MA powder, which has a lower O percentage most probably due to the lower oxygen percentage of the HDH powder used to fabricate it (Table 3). Carbon content is significantly lower for the prealloyed powders (Ti64-PA and Ti32-PA) than for the powders produced from master alloy addition, due to the wax used as PCA during milling that remains mixed with the powder (*see* Table 3). The Ti32-MA alloy, which has half of the amount of master alloy as compared to the Ti64-MA alloy, has approximately half the C content of the Ti64-MA alloy.

Table 3 Chemical analysis and particle size distribution of HDH titanium and fabricated Al/V (60 : 40) used as starting materials to obtain desired final alloys

Material		Ti	Al/V (60 : 40)
Chemical analysis	O, wt-%	0·272	1·16
	N, wt-%	0·0159	0·0384
	C, wt-%	0·0202	0·792
Particle size analysis	D_{max}, μm	<75	<63
	D_{10}, μm	17·31	2·46
	D_{50}, μm	37·59	12·61
	D_{90}, μm	72·59	55·81

The densities of the PA powders measured by the helium pycnometer, which were kept as references for the calculation of the relative density, are similar to the values found in the literature for the wrought products (4·43 and 4·48 g cm^{-3} for Ti–6Al–4V and Ti–3Al–2·5V respectively).[17] Compared to PA powders, the densities of the MA powders are somewhat lower, which is probably due to the fact that, during these measurements, the powders still contained the wax used as PCA for the milling of the master alloy.

Measurements of the apparent densities and flowrates by means of the Hall apparatus failed due to the morphology of the powder. The apparent densities were therefore measured by Carney apparatus with the help of a wire to agitate the powder to promote powder flow (MPIF 28). The values obtained are very similar for the two PA powders and lower than those for the MA powders. This observation can be explained based on the particle size distribution of the milled master alloy and the pure titanium starting powder shown in Table 3. Because the master alloy has a slightly lower particle size than HDH Ti, its particles fitted in between the bigger particles, leading to better packing and, therefore, higher apparent densities.

Scanning electron microscopy was used to examine the morphology and microstructure of the powders (Figs. 2 and 3).

Both the prealloyed and master alloyed titanium powders were obtained by the HDH method; hence, they are angular or even irregular in shape (Fig. 2), which accounted for why they do not flow in the Hall apparatus.

During the microstructure analysis of previously grinded, polished and etched samples, the various elements in the final alloy, namely, pure titanium, pure aluminium and master alloy, were identified by means of the energy dispersive spectroscopy technique (Fig. 3).

The microstructure of the Ti64-PA consist of equiaxial α and $\alpha+\beta$ grains, as expected from the composition. The Ti32-PA powder was obtained by mixing Ti64-PA powder with elemental Ti powder, as shown in Fig. 3*a*, where the two types of particles with slightly different contrasts can be distinguished. In the image corresponding to the Ti64-MA alloy (Fig. 3*b*), the powders that composed the alloy can be seen. The brightest particles

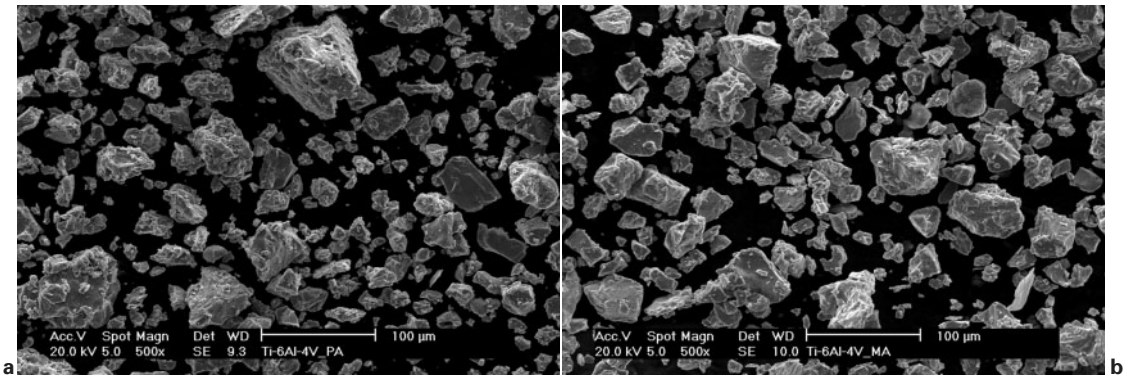

a b

2 Morphologies as determined by SEM for *a* Ti64-PA and *b* Ti64-MA powders

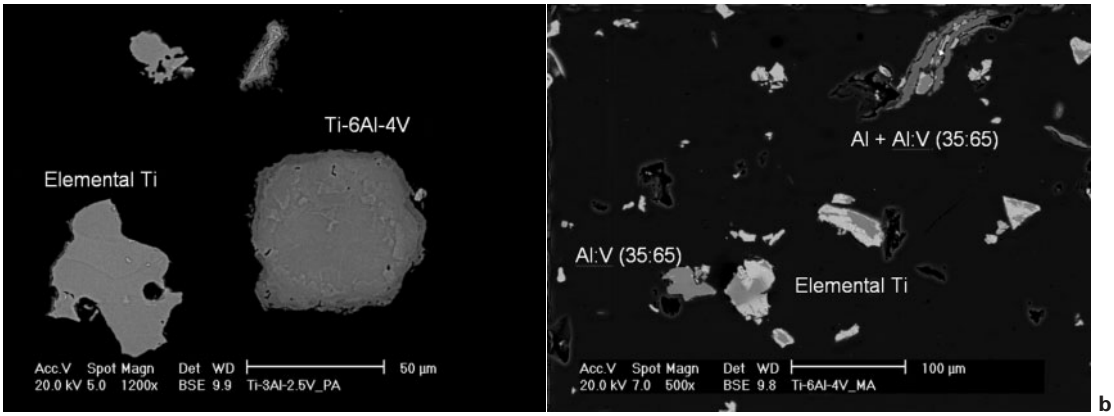

a b

3 Scanning electron microscopy metallographic cross-sections of *a* Ti32-PA and *b* Ti64-MA powders

with dark shadows correspond to pure titanium, the darkest particles correspond to pure Al or Al mixed with the Al/V master alloy, and the grey particles correspond to the master alloy Al/V (35 : 65). The individual elements are still distinguishable because the Ti64-MA and Ti32-MA alloys were produced by conventional blending, and the milling was carried out only to reduce its particle size and adjust the final composition and not to produce a master alloy or a prealloyed powder.

Compressibility test was performed for the different powders by varying the pressure from 300 to 700 MPa, and the results obtained are shown in Fig. 4.

From Fig. 4, it can be seen that the PA powders have lower compressibility than MA, as expected. The PA powders are much more brittle and less deformable because the alloying elements are already dissolved into the Ti. However, it is interesting to note that the Ti32-PA powder, which was fabricated by mixing elemental HDH Ti powder and Ti64-PA powder, has lower compressibility than the Ti64-PA powder. This lower compressibility is due to the small mismatch in particle size distribution between the raw powders and the slightly lower nitrogen content[18,19] of the Ti64-PA powder compared to the elemental Ti powder. The Ti32-MA powder has a better behaviour under pressure than the Ti64-MA powder, which can be related to the better apparent density or the lower oxygen content[18,19] of the Ti32-MA alloy. In this case, the carbon content does not affect the compressibility and mechanical properties of the powders because it is not dissolved in the material. A good compressibility is one of the most important factors for powders to be used in conventional PM routes because the higher the green density, the lower the shrinkage of the part during sintering, which results in a smaller dimensional change in the final shape of a component.

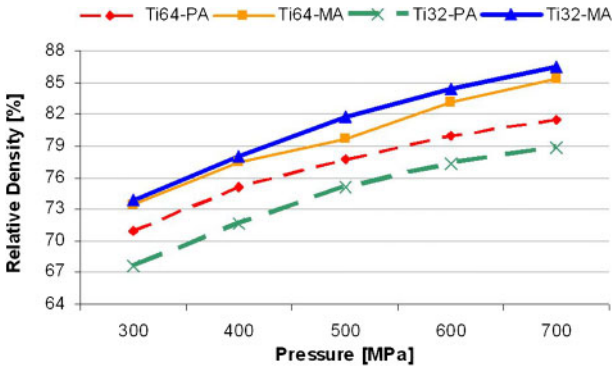

4 Compressibility curves of powders studied

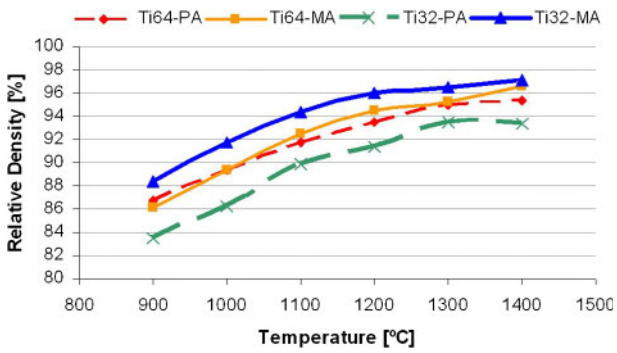

5 Relative density versus sintering temperature

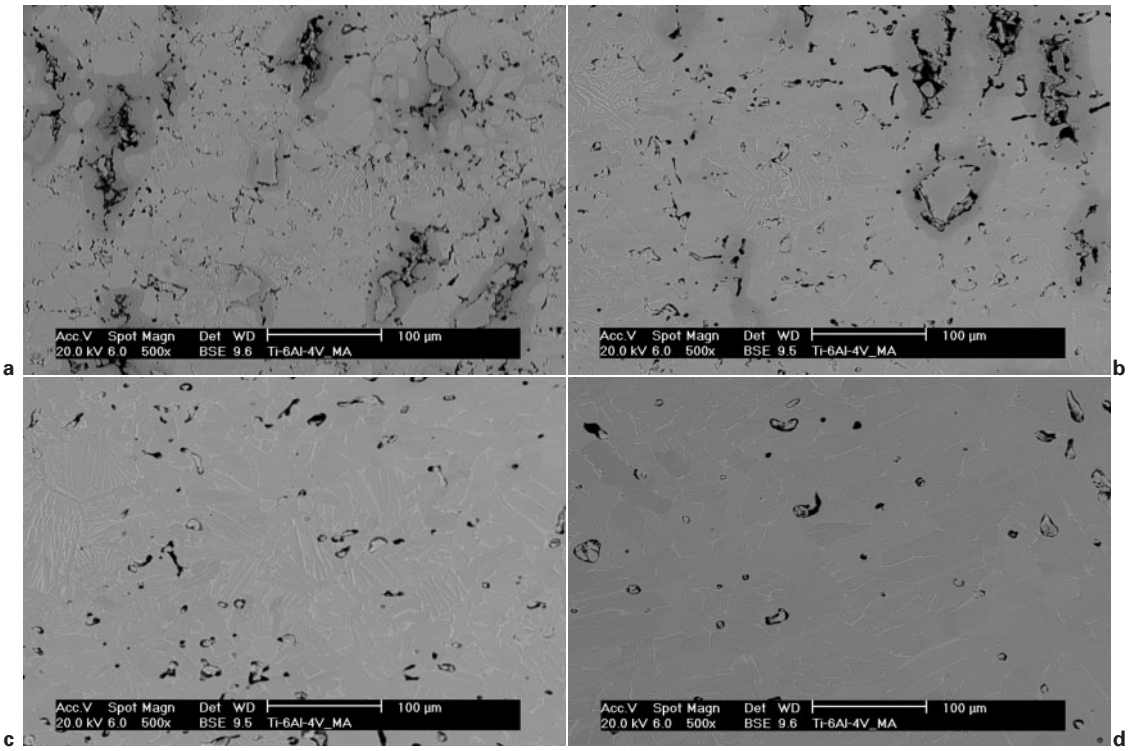

a 900°C; *b* 1000°C; *c* 1100°C; *d* 1200°C

6 Evolution of microstructure with sintering temperature for Ti64-MA alloy analysed by backscattered electron

A three-point bending test was used to determine the green strength as a function of the consolidation pressure for the titanium alloy powders. Ranging the pressure from 300 to 700 MPa, the green strength increases from 5 to 25 MPa. As expected, the green strength increases with the compaction pressure, and the strengths obtained guarantee the handling of the components even at 300 MPa.

Based on the results shown, an optimum compaction pressure of 700 MPa was chosen for the MA powders, whereas the compaction pressures were limited to 400 and 300 MPa for Ti64-PA and Ti32-PA respectively. This limitation was dictated by the need to avoid fracturing at the corner or delamination phenomena on the bottom of the specimens, as well as to lower the friction and the wear with the wall of the die.

Sinterability study

Once the compaction pressure was optimised, the powders were uniaxially cold pressed into specimens with the shape and dimensions normalised for three-point bending test and sintered under the same conditions between 900 and 1400°C. In the case of the MA powders, a dwell time of 30 min at 300°C was employed to eliminate the wax used as PCA during milling.

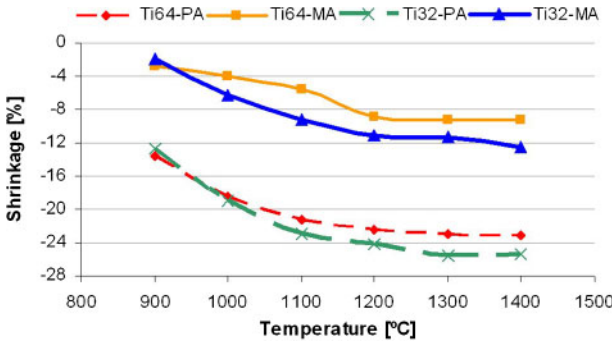

7 Dimensional change of alloys studied as function of sintering temperature

Figure 5 shows the results of the relative density versus the sintering temperature for the processed materials.

As expected, the relative density of the samples (Fig. 5) increases with the sintering temperature, reaching the maximum value at the highest temperature and showing an asymptotic behaviour. Generally, the typical relative density for titanium PM samples processed by conventional techniques (94%)[14,20] can be obtained by selecting a specific sintering temperature for each of the alloys investigated. Titanium alloys produced from MA powders reached slightly higher densities than PA powders because they started from a higher green density.

A study of the evolution of the microstructure with the sintering temperature was conducted by SEM, and some results are reported in Fig. 6.

From Fig. 6, it can be seen that at low temperatures, the alloying elements, either master alloy or elemental powder, are not completely diffused through the titanium matrix, but once sintering temperature is above 1100°C, the alloying elements are completely diffused as backscattered electron SEM images and XRD analysis confirm. Moreover, at this processing temperature, there are already distinguishable white α/β grain boundaries because it is higher than 996°C, the nominal β transus temperature for the Ti–6Al–4V alloy.[17] The same behaviour for the evolution of the microstructure was found for Ti32 alloys, and it is reasonable considering that the relative percentage of alloying elements that has to diffuse is lower. There were no issues of undiffused

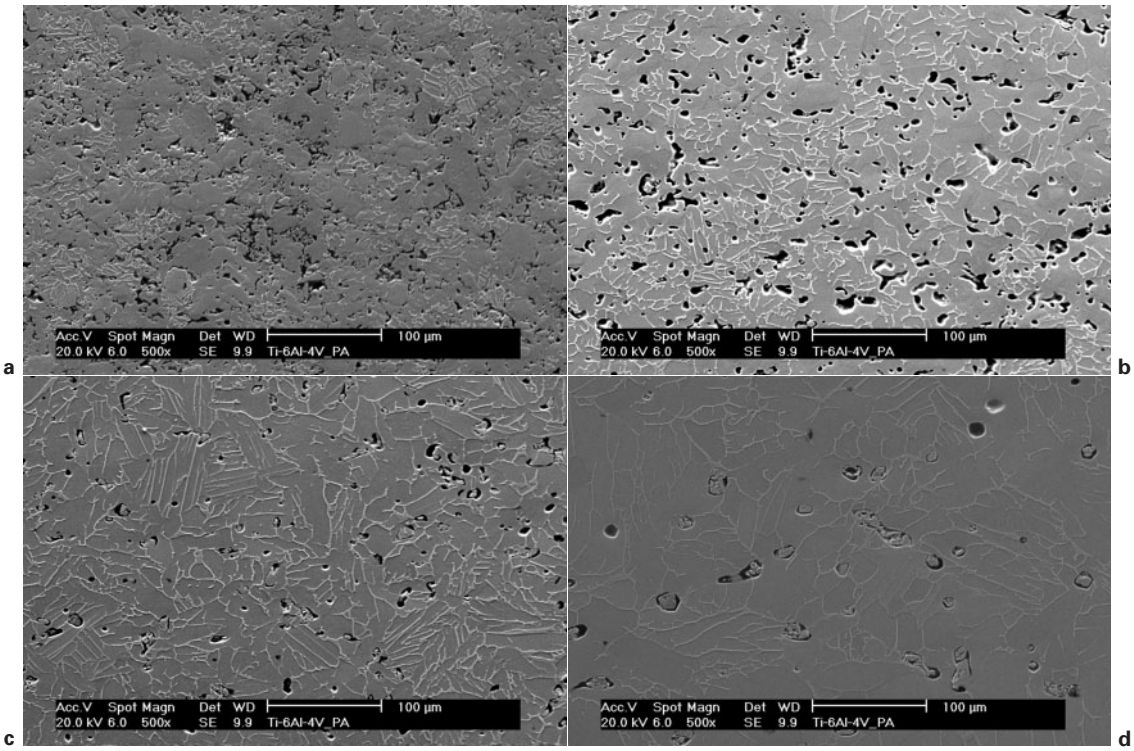

a 900°C; *b* 1000°C; *c* 1100°C; *d* 1400°C

8 Images (SEM) in secondary electron mode, showing residual porosity of Ti64-PA alloy sintered at different temperatures

elements with the prealloyed powder because each particle already has the final desired composition.

Even though the specimens were compacted at different pressures, they reached comparable final relative density values. Hence, the shrinkage induced by sintering, which is shown in Fig. 7, was analysed.

As shown in Fig. 7, the shrinkage of titanium alloys increases with the sintering temperature, but there is a less significant increment when raising the temperature from 1200 to 1400°C, which could indicate that a great amount of thermodynamic energy available is spent to promote grain growth instead of densification above 1200°C. Moreover, it is worth mentioning that the PA materials show much higher volume shrinkage (as high as 25%) than the MA materials, and the Ti32-PA alloy exhibited slightly higher volume shrinkage than the Ti64-PA alloy due to the lower compaction pressure used.

Figure 8 shows the residual porosity as well as microstructural features for the Ti64-PA alloy sintered at different temperatures analysed by SEM in the secondary electron mode.

At 900°C (Fig. 8*a*), the formation of the sintering necks is still under development, the boundaries between different particles are still visible and the porosity is mostly interconnected. At 1000°C (Fig. 8*b*), the interparticle boundaries are no longer distinguishable, and the residual porosity is still interconnected and completely irregular in shape. At 1100°C (Fig. 8*c*), the total porosity is much lower and the pores are isolated and more spherical. At 1400°C (Fig. 8*d*), the percentage of residual porosity decreases, which is in agreement with the relative density results, but the pores are bigger in size, predominantly spherical in shape and isolated, which is the typical behaviour of the intermediate stage of sintering.[21] From the microstructural analysis, it also

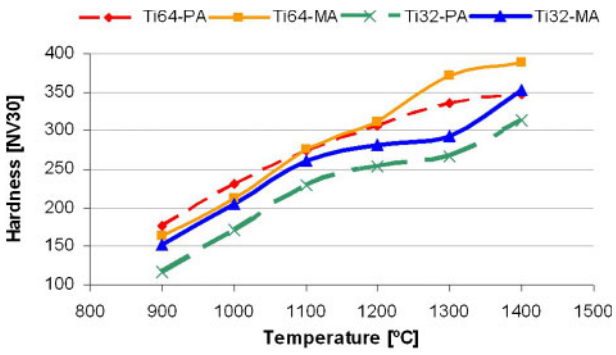

9 Hardness HV30 of alloys studied as function of sintering temperature

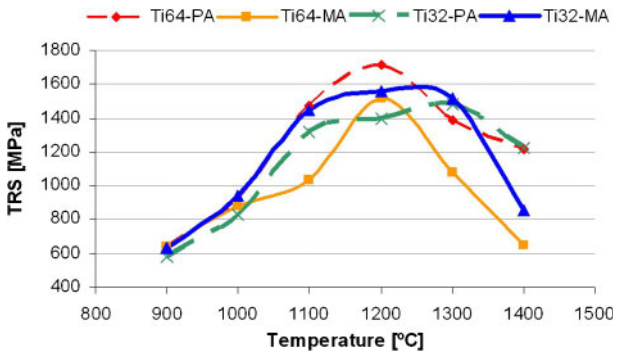

10 Transverse rupture strength as function of sintering temperature

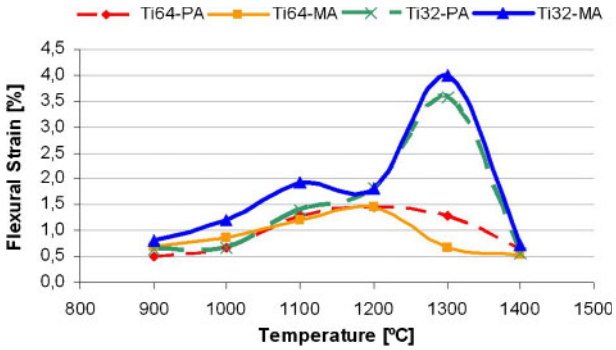

11 Flexural strain obtained in three-point bending test versus sintering temperature

seems that increasing the temperature from 1100 to 1400°C results in grain growth.

Another indicative property that can be used to monitor the evolution of a PM material with the sintering temperature is the hardness. In this work, the HV30 hardness was considered, and the results are shown in Fig. 9.

As expected, the hardness (Fig. 9) increases with the processing temperature in exactly the same manner as the relative density, and the MA alloys reach higher hardness values, indicating that the MA approach is an economical and viable way to obtain cheaper titanium products.

For both the Ti64 and Ti32 alloys, independent of the powder production method, a minimum temperature of 1200°C has to be reached to achieve the hardness of the wrought products, which is equivalent to 330 and 260 HV30 for the Ti64 and Ti32 alloys respectively.[17,22]

This result is remarkable because a 1200°C sintered alloy corresponded to a material with ~92% of relative density (Fig. 5) where the microstructure is fully developed (Fig. 6), instead of a fully dense wrought material. The high hardness of the less dense alloy is most probably related to the higher oxygen content of the starting powder compared to the nominal composition of these alloys.[17,22]

The TRS obtained by the three-point bending test and the maximum flexural strain are presented as a function of the sintering temperature in Figs. 10 and 11 respectively.

The strength (Fig. 10) of the sintered materials increases with the processing temperature, but there is a drop above 1200 and 1300°C for the Ti64 and Ti32 alloys respectively. This drop is most probably due to grain growth at higher temperatures, which lowers the strength, since the shrinkage is almost constant above 1200°C (Fig. 7), and therefore, the thermal energy promoted grain growth instead of densifying the material. When comparing the production routes, it can be seen that the Ti64-PA has a better mechanical strength than Ti64-MA, and Ti32-MA alloy has a higher resistance than Ti32-PA. This result can be explained by considering the amount of interstitial elements[18,19,23] of the starting powders, especially the oxygen content. The maximum TRS values ranged from 1500 to 1700 MPa, and minimum TRS values of ~600 MPa were obtained.

From Fig. 11, it can be seen that flexural strain increases up to a certain temperature (1200°C for Ti64 alloys and 1300°C for Ti32 alloys), and then it drops. It is well known that the ductility of titanium is significantly influenced by the chemical composition,

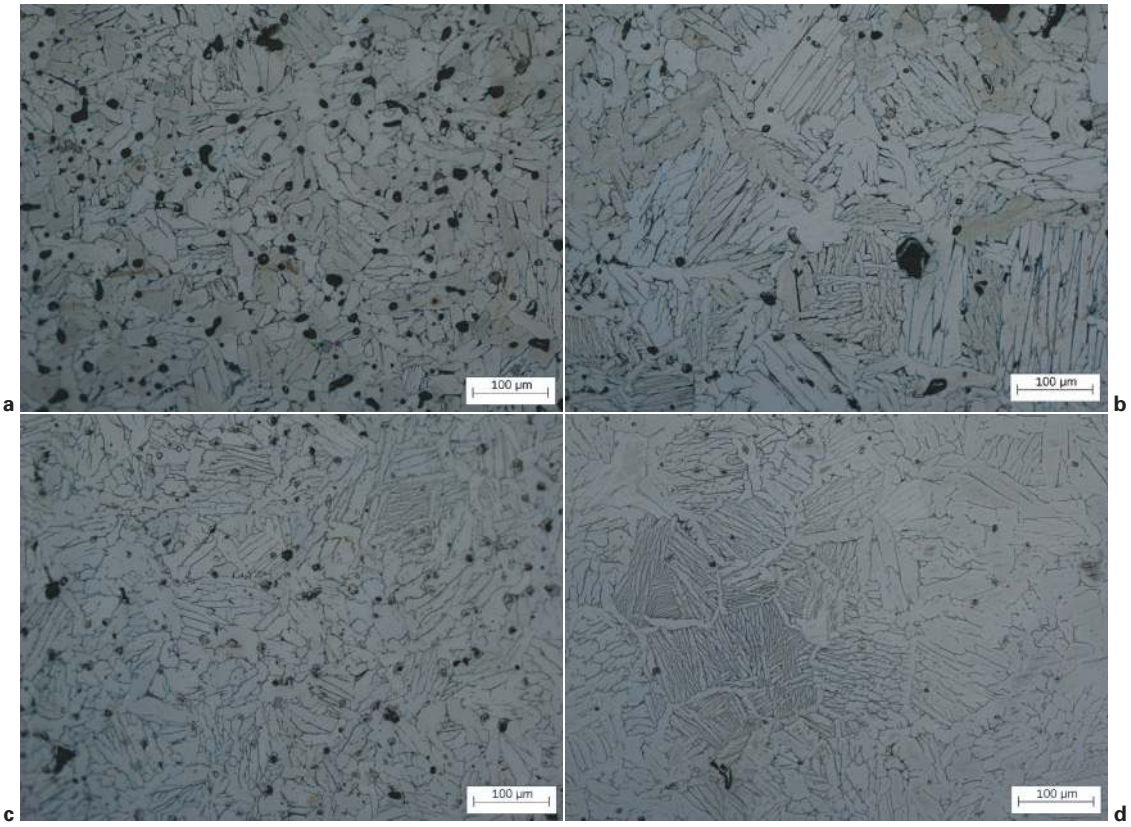

a Ti64-PA; *b* Ti64-MA; *c* Ti32-PA; *d* Ti32-MA

12 Microstructure obtained by light optical microscopy of materials sintered at 1200°C

where the lower the oxygen content, the higher the ductility, but the drop in the material deformation at the highest temperatures could also be related to the grain growth. For the Ti–3Al–2·5V alloys sintered at 1300°C, a flexural strain as high as 3·5–4% was obtained, which is very promising, and further tensile test investigations should be conducted.

Finally, Fig. 12 shows optical microscopy microstructure images of an etched specimen for each alloy.

The optical microscopy study shows that, for temperatures higher than 1100°C, the typical lamellar microstructure of near α and $\alpha+\beta$ titanium alloys is fully developed and composed of large α grains and acicular $\alpha+\beta$ lamellae at the grain boundaries.[24] Moreover, when comparing the powder production routes, it can be seen that PA alloys are characterised by smaller and thicker basket weave or Widmanstätten areas, and their percentage is significantly lower than that of the MA alloys. Uniform and homogeneous microstructures were obtained regardless of the alloy or the production method.

Conclusions

Ti–6Al–4V and Ti–3Al–2·5V titanium alloys were either purchased or produced by the master alloy blending elemental approach using a HEM step to adjust the composition and the particle size of the master alloy used as raw material. The following conclusions can be stated.

1. The chemical compositions of all the alloys are very similar. Only Ti–3Al–2·5V produced by the master alloy approach has a slightly lower oxygen content. The powders fabricated by master alloy addition have a higher percentage of C, primarily due to the production route employed. However, this element does not affect the compressibility or the mechanical properties in the green state because it is not dissolved inside the matrix.

2. Alloys produced by the blending elemental approach, in particular by master alloy addition, have better compressibility because the prealloyed powders are harder due to the formation of a solid solution. Nonetheless, no significant differences were found in terms of the green strength, and the green products can be handled without problems in the range of compaction pressures investigated.

3. A minimum temperature of 1100°C has to be reached to guarantee complete diffusion of the alloying elements in the case of master alloy addition.

4. The constituents of the microstructure are α grains of different sizes and orientations and $\alpha+\beta$ lamellae placed at the grain boundaries typical of the Widmanstätten microstructure. For master alloy addition alloys, the basket weave areas are higher in relative amount, bigger in total size and lower in lamella thickness because the alloying elements have to diffuse inside the matrix, which used up energy normally available to form equilibrium phases.

5. Transverse rupture strength and flexural strain increase with the sintering temperature up to a specific temperature (1200 and 1300°C for Ti–6Al–4V and Ti–3Al–2·5V respectively) and then drop markedly, most probably due to the grain growth induced by the increase in the processing temperature.

Acknowledgements

The authors would like to acknowledge the financial support from the Spanish Ministry of Education through R&D projects nos. MAT2009-14448 and MAT2009-14547 and from Comunidad de Madrid through the ESTRUMAT (grant no. S2009/MAT-1585) project.

References

1. W. J. Kroll: *Z. Anorg. Chem.*, 1937, **234**, 422.
2. S. J. Gerdemann: 'Titanium process technologies', *Adv. Mater. Process.*, 2001, **159**, 41–43.
3. G. Crowley: 'How to extract low-cost titanium', *Adv. Mater. Process.*, 2003, **161**, 25–27.
4. G. Z. Chen, D. J. Fray and T. W. Farthing: 'Direct electrochemical reduction of titanium dioxide to titanium in molten calcium chloride', *Nature*, 2000, **407**, 361–364.
5. C. M. Ward-Close, A. B. Godfrey and S. R. Thompson: 'Titanium made the EDO way should see prices drop', *Met. Powder Rep.*, 2005, **60**, 20–25.
6. W. Schatt and K.-P. Wieters: 'Powder metallurgy processing and materials'; 1997, Shrewsbury, EPMA.
7. C. M. WardClose, A. B. Godfrey and S. R. Thompson: 'Advances in titanium alloy powder', Proc. Conf. Euro PM 2004, 261–266; 2004, European Powder Metallurgy Association, Vienna.
8. A. Alagheband and C. Brown: 'Plasma atomization goes commercial', *Met. Powder Rep.*, 1998, **53**, 26–28.
9. M. Mitkov and D. Božić: 'Hydride–dehydride conversion of solid Ti6Al4V to powder form', *Mater. Charact.*, 1996, **37**, 53–60.
10. V. A. Druz, V. S. Moxson, R. Chernenkoff, W. F. Jandeska, Jr and J. Lynn: 'Blending an elemental approach to volume titanium manufacture', *Met. Powder Rep.*, 2006, **61**, 16–21.
11. P. J. Andersen and P. C. Eloff: 'Development of higher performance blended elemental powder metallurgy Ti alloys', Proc. Conf. on 'Powder metallurgy of titanium alloys', Las Vegas, NV, USA, February 1980, AIME, 175–187.
12. J. E. Smugeresky and D. B. Dawson: 'New titanium alloys for blended elemental powder processing', *Powder Technol.*, 1981, **30**, 87–94.
13. O. M. Ivasishin, V. M. Anokhin, A. N. Demidik, and D. G. Savvakin: 'Cost-effective blended elemental powder metallurgy of titanium alloys for transportation application', *Key Eng. Mater.*, 2000, **188**, 55–61.
14. F. H. Froes, O. M. Ivasishin, V. S. Moxson, D. G. Savvakin and K. A. Bondareva: 'Cost-effective synthesis of Ti–6Al–4V alloy components via the blended elemental P/M approach', Proc. Symp. on 'High performance P/M components', Coimbra, Portugal, April–May 2002, UEF. 1–12.
15. J. Park, M. W. Toaz and D. H. Ro: 'Forming of near net shapes of titanium alloys by blended elemental powder metallurgy', *Ind. Heat.*, Dec. 1984, 32–35.
16. T. Fujita, A. Ogawa, C. Ouchi and H. Tajima: 'Microstructure and properties of titanium alloy produced in the newly developed blended elemental powder metallurgy process', *Mater. Sci. Eng. A*, 1996, **A213**, 148–153.
17. RMI Titanium Company: 'Titanium alloy guide'; 2000, http://rtiintl.s3.amazonaws.com/RTI-Reports/tiguideWeb.pdf.
18. R. I. Jaffee, H. R. Ogden and D. J. Maykuth: 'Alloys of titanium with carbon, oxygen and nitrogen', *Trans. Am. Inst. Mining Metall. Eng.*, 1950, **188**, 1261–1266.
19. R. I. Jaffee and I. E. Campbell: 'The effect of oxygen, nitrogen and hydrogen on iodide refined titanium', *Trans. Am. Inst. Mining Metall. Eng.*, 1949, **185**, 646–654.
20. S. Abkowitz and D. Rowell: 'Superior fatigue properties for blended elemental P/M Ti–6Al–4V', *JOM*, 1986, **39**, 36–39.
21. R. M. German: 'Powder metallurgy science', 2nd edn; 1994, Princeton, NJ, MPIF.
22. R. Boyer, G. Welsch and E. W. Collings: 'Materials properties handbook: titanium alloys', 2nd edn; 1998, Materials Park, OH, ASM International.
23. W. L. Finlay and J. A. Snyder: 'Effects of three interstitial solutes (nitrogen, oxygen and carbon) on the mechanical properties of high-purity, alpha titanium', *J. Met.*, 1950, **188**, 277–286.
24. G. Lütjering and J. C. Williams: 'Titanium: engineering materials and processes', 1st edn; 2003, Berlin/Heidelberg/New York, Springer.